Available online at www.sciencedirect.com

SciVerse ScienceDirect

Ceramics International 38 (2012) 6123–6129

CERAMICS INTERNATIONAL

www.elsevier.com/locate/ceramint

Preparation of TiO_2/carbon nanotubes photocatalysts: The influence of the method of oxidation of the carbon nanotubes on the photocatalytic activity of the nanocomposites

Veljko R. Djokić[a,*], Aleksandar D. Marinković[a], Miodrag Mitrić[b], Petar S. Uskoković[a], Rada D. Petrović[a], Velimir R. Radmilović[c], Djordje T. Janaćković[a]

[a]*Faculty of Technology and Metallurgy, University of Belgrade, Karnegijeva 4, 11120 Belgrade, Serbia*
[b]*Condensed Matter Physics Laboratory, Vinča Institute, University of Belgrade, P.O. Box 522, 11001 Belgrade, Serbia*
[c]*Nanotechnology and Functional Materials Center, Faculty of Technology and Metallurgy, University of Belgrade, Karnegijeva 4, 11120 Belgrade, Serbia*

Received 28 February 2012; received in revised form 20 April 2012; accepted 21 April 2012
Available online 3 May 2012

Abstract

A method for the preparation of efficient TiO_2/multi-wall carbon nanotubes nanocomposite photocatalysts by precipitation of anatase TiO_2 nanoparticles onto differently oxidized carbon nanotubes is presented. The precursor compound titanium(IV) bromide was hydrolyzed producing pure anatase phase TiO_2 nanoparticles decorated on the surface of the oxidized carbon nanotubes. The oxidative treatment of the carbon nanotubes influenced the type, quantity and distribution of oxygen-containing functional groups, which had a significant influence on the electron transfer properties, *i.e.*, the photocatalytic activity of the synthesized nanocomposites. The results of C.I. Reactive Orange 16 photodegradation in the presence of all the synthesized nanocomposites showed their better photocatalytic activity in comparison to the commercial photocatalyst Degussa P-25.

Keywords: A. Sol–gel processes; B. Nanocomposites; D. TiO_2; E. Photocatalysis

1. Introduction

Titania (TiO_2) is one of the most widely studied semiconductors for environmental protection, self-cleaning, deodorizing and sterilizing applications due to its low cost, abundant resource, photocatalytic activity, harmlessness and resistance to chemical corrosion and photocorrosion. However, in order to provide high photocatalytic activity, as proved by numerous studies, it is necessary to synthesize titania of high: specific surface area, crystallinity, porosity, extended lifetime of the photon-generated electron–hole pairs, *etc*. [1–4].

One approach for enhancing the photocatalytic activity of TiO_2 was achieved by the synthesis of novel nanostructured carbonaceous composite materials by controlling their structural and electron transfer properties. In recent reviews [3,5], attention was paid to the fact that carbon nanotubes (CNT) are attractive and promising candidates for improving the photocatalytic efficiency of TiO_2 due to the contribution of their exceptional electronic, adsorption, mechanical and thermal properties, chemical inertness and stability. TiO_2 is an *n*-type semiconductor and the main process in photocatalysis is activated by photon absorption and electron–hole generation. Therefore, an enhancement of the photocatalytic properties of TiO_2 could be achieved in conjunction with functionalized CNT, which promote electron–hole pair separation and migration; a process that leaves an excess of holes in the valence band and the photogenerated electrons move freely from the conduction band of the TiO_2 to the electron-accepting CNT surface. In this way, TiO_2 effectively behaves as a *p*-type semiconductor in TiO_2/CNT nanocomposites. Additionally, the large number of active adsorption sites at the catalyst surface and the improved suppression of

*Corresponding author. Tel.: +381 64 270 1090; fax: +381 11 3370 387.
E-mail addresses: vdjokic@tmf.bg.ac.rs, djokicveljko@yahoo.com (V.R. Djokić).

0272-8842/$36.00
http://dx.doi.org/10.1016/j.ceramint.2012.04.060

the recombination of the charge carriers contribute to the higher photocatalytic activity [3,5].

Many specific methods for the synthesis of TiO_2/CNT nanocomposites have been developed, which generally consist of two steps: functionalization of the CNT and nanocomposite synthesis. One of the functionalization methods applied to CNT is oxidative treatment, upon which the nanotubes become shortened, less tangled and their ends opened, and oxygen-containing functional groups are introduced on their surface. Those groups have a pronounced effect on the surface properties of the carbonaceous material, providing numerous sites for TiO_2 bonding. It was shown that oxidative treatment introduces different hydrophilic functional groups on the CNT surface, but does not provide sufficient control over their number, type and location. Additionally, it was explained that the distribution of the oxygen-containing functional groups is very sensitive to the type of oxidant [6–9].

Therefore, the aim of this work was to prepare nanocomposite photocatalysts, by precipitation of TiO_2 on differently oxidized multi-wall carbon nanotubes (MWCNT) in order to study the effect of oxidative methods on the photocatalytic activity of the obtained composites. The photocatalytic activity was studied employing the reaction of the photoactivated degradation of the textile dye C.I. Reactive Orange 16, and obtained results are discussed in relation to the factors contributing to the enhanced photoactivity.

2. Materials and methods

2.1. Preparation of nanocomposite photocatalyst

Titanium tetrabromide (98%, Acros Organics), MWCNT (95+%, Aldrich), absolute ethanol and other chemicals (Fluka, p.a.) were used as received. Millipore deionized (DI) water (18 MΩ cm resistivity) was used for sample washing and solution preparation.

The oxidized MWCNT were prepared according to a modified literature method published elsewhere [6]: MWCNT1: MWCNT (100 mg) were sonicated (Sonorex) in 200 cm^3 of 65% HNO_3 for 1 h, followed by refluxing for 1.5 h at 140 °C. MWCNT2: $KMnO_4$ (200 mg) was dissolved in 200 cm^3 of 0.5 mol dm^{-3} H_2SO_4. MWCNT (100 mg) was sonicated in 200 cm^3 of 0.5 mol dm^{-3} H_2SO_4 for 30 min and after heating to 150 °C, the $KMnO_4$ solution was added slowly. The MWCNT/$KMnO_4$ dispersion was refluxed for 5 h at 150 °C. HCl (10 cm^3 of 35%) was added to the cooled reaction mixture to dissolve the MnO_2 byproduct. MWCNT3 and MWCNT4: MWCNT (100 mg) were added to 120 cm^3 (H_2SO_4 (98%)/HNO_3 (65%) v/v 3:1) solution and then sonicated at 40 °C for 3 h (MWCNT3) or 6 h (MWCNT4). All products were purified by centrifugation, washed with deionized water and vacuum-filtered using a 0.05 μm polytetrafluoroethylene (PTFE) membrane filter. Before the preparation of the photocatalysts, the oxidized MWCNTs were dried in a vacuum oven at 80 °C for 120 min.

TiO_2 precipitation onto the oxidized MWCNTs was performed by hydrolysis of titanium tetrabromide according to a literature method developed by Németh et al. [10]. In the case of MWCNT4, the TiO_2/MWCNT ratio was changed in order to obtain the optimal ratio of TiO_2 and MWCNT. Different amounts of MWCNT4 (0, 5, 10, 15, 20, 25 and 30 mg) were dispersed in absolute ethanol (1.6 cm^3) and then 1.1 mmol $TiBr_4$ was added and the dispersion sonicated for 60 min under a nitrogen atmosphere. $TiBr_4$ hydrolysis was achieved by addition of 0.32 cm^3 deionized water. The products were dried at 110 °C for 2 h, heated to 400 °C at a rate of 10 °C/min and calcined for 30 min. The other nanocomposites, TiO_2/MWCNT1, TiO_2/MWCNT2 and TiO_2/MWCNT3, were prepared using the optimal ratio found for the TiO_2/MWCNT4 photocatalyst.

2.2. Characterization

The specific surface area and pore volume were measured using Micromeritics ASAP 2020 surface area analyzer. X-Ray diffraction (XRD) data were obtained using a BRUKER D8 ADVANCE with a Vario 1 focusing primary monochromator ($Cu_{k\alpha 1}$ radiation, $\lambda = 1.54059$ Å). The crystallite size of anatase was determined according to the Scherrer equation:

$$D = K\lambda/(\beta \cos \theta)$$

where λ is the wavelength of the X-ray radiation ($\lambda = 1.54059$ Å), K is the Scherrer constant ($K = 0.9$), θ is the angle of characteristic X-ray diffraction peak ($\theta = 12.65°$) and β is the full-width-at-half-maximum of the anatase (101) plane (in radians). Scanning electron microscopy (FEG–SEM) was performed with field emission gun TESCAN MIRA3 electron microscope. A diameter of nanocomposites was determined using of MIRA TESCAN in-situ measurement software. Conventional transmission electron microscopy (CTEM) was performed using an AEM JEOL 200CX microscope at 200 kV, and high resolution transmission electron microscopy (HRTEM) using a TEAM0.5 aberration corrected electron microscope operated at 80 kV, below threshold for knock-on damage of the CNT [11]. The atomic compositions of the obtained materials were determined by electron energy-loss spectroscopy (EELS) in the scanning TEM (STEM) mode. The Boehm method [12] was applied for the determination of type and quantity of functional groups present on the surface of the oxidized MWCNT.

2.3. Photocatalytic activity

Photocatalytic decomposition of the textile dye C.I. Reactive Orange 16 (Bezema) was followed by decrease of the absorbance of aqueous dye solution (50 mg dm^{-3}) in the presence of the synthesized photocatalysts or the commercial P25 photocatalyst (50 mg in 25.0 cm^3 of solution). The dispersions were mixed in the dark for

30 min in order to establish adsorption/desorption equilibrium and then illuminated with UVA light using a Philips 125 W lamp with an intensity of 12.7 mW/cm^2. Samples (3.0 cm^3) were taken and separated from the photocatalysts by filtration (0.2 μm poly(vinylidene fluoride) (PVDF) syringe filter, Whatman) and used for the determination of time-dependent change in the dye concentration employing a Shimadzu 1800 UV–vis spectrophotometer. The light irradiation intensity was measured by a UVX Digital Ultraviolet Intensity Meter (Cole-Parmer, USA; Model: 97-0015-02(UVX)) using a 365 nm sensor (97-0016-02(UVX36)). The durability of all nanocomposite catalysts was checked in five consecutive cycles. After each cycle, the catalyst was recovered by centrifugation, washed with ample DI water, dried at 80 °C or calcined (400 °C for 15 min), and reused in the next degradation cycle.

3. Results and discussion

3.1. Characterization of the samples

The results of the Boehm titration of raw and oxidized MWCNTs are shown in Table 1. Different MWCNT oxidative treatment routes lead to the increased content of oxygen-containing functional groups in following order: MWCNT1 < MWCNT2 < MWCNT3 < MWCNT4. Six hours of oxidative treatment increased the contribution of carboxyl groups by ≈20% and the total oxygen acidic groups by about 10%, compared to MWCNT3. Prolonged oxidative treatment of the MWCNTs caused more intensive degradation of the graphitic structure, mainly at the nanotube ends, and graphitic plane opening created sidewall defect sites [6].

According to the results of photocatalytic activity of nanocomposites obtained with different ratios of TiO_2 and MWCNT4 (data not shown), the highest photocatalytic activity was obtained with 19 wt% of MWCNT4 (20 mg and 1.1 mol $TiBr_4$). This optimal ratio was used for preparation of all nanocomposites. Higher MWCNT loadings led to an increased shielding of the active photocatalytic sites, as well as increased absorbance and scattering of photons, resulting in a decrease in the photocatalytic activity.

The specific surface area (S_p) and pore volume (V_p) of the raw, oxidized MWCNTs, and of the nanocomposites are given in Table 2. In addition, the data for pure TiO_2, obtained by $TiBr_4$ hydrolysis without MWCNT, are presented. Highest surface area was found for the raw MWCNT, significantly lower for the oxidized MWCNTs and the lowest for the nanocomposites. Specific surface areas of MWCNT1 and MWCNT2 were higher than those of MWCNT3 and MWCNT4 due to the milder oxidative treatment. The decrease in the surface area and pore volumes was due to the smaller confined space among the oxidized MWCNTs [13] and the introduction of oxygen-containing functional groups [6], as well as to the heterogeneous nucleation of TiO_2 at defect sites during the production of the nanocomposites. Additionally, the surface area and pore volume of pure TiO_2 were lower (Table 2) than those of the synthesized nanocomposites, providing additional evidence that precipitation of TiO_2 contributed to the decreases of the overall surface area of all the nanocomposites. Similar trend of the pore volume (V_p) changes to those found for the specific surface area was observed for all the nanocomposites.

Table 1
Results of the Boehm titration.

	Carboxyls (mmol g^{-1})	Lactones (mmol g^{-1})	Phenols (mmol g^{-1})	Total acidic sites (mmol g^{-1})	Total basic sites (mmol g^{-1})
MWCNT	0.07	0.28	0.24	0.58	0.19
MWCNT1	0.82	1.54	1.22	3.58	0.36
MWCNT2	0.85	1.62	1.31	3.78	0.38
MWCNT3	0.87	1.78	1.43	4.09	0.42
MWCNT4	1.04	1.88	1.57	4.49	0.40

Table 2
Specific surface area (S_p) and pore volume (V_p) of the raw and oxidized MWCNT, nanocomposites and pure TiO_2.

Sample	S_p, m^2 g^{-1}	V_p, cm^3 g^{-1}
MWCNT	187.582	0.755
TiO_2/MWCNT	144.852	0.167
MWCNT1	102.356	0.485
TiO_2/MWCNT1	76.741	0.101
MWCNT2	96.253	0.464
TiO_2/MWCNT2	79.584	0.098
MWCNT3	78.492	0.328
TiO_2/MWCNT3	62.238	0.070
MWCNT4	76.167	0.277
TiO_2/MWCNT4	61.690	0.063
TiO_2 Pure	32.735	0.031

The X-ray diffraction (XRD) patterns of the synthesized nanocomposite photocatalysts, presented in Fig. 1, showed that TiO_2 in the nanocomposite is in the anatase phase, while the pure TiO_2 contained a negligible quantity of rutile phase. This suggests that the MWCNTs suppressed the anatase to rutile phase transformation during calcination [14].

According to the XRD analysis and applying the Scherrer equation, a slight dependence of the crystallite size with respect to the MWCNT oxidation method was found in all the samples (Table 3).

For a better understanding of the interaction between TiO_2 and the surface of oxidized MWCNT, the morphology and nanostructure of the sample TiO_2/MWCNT4 were studied by the FEG–SEM and TEM/HRTEM techniques (Fig. 3) and compared with those of TiO_2/MWCNT (Fig. 2). The FEG–SEM micrograph (Fig. 2), revealed that TiO_2/MWCNT4 (Fig. 2b), compared to TiO_2/MWCNT (Fig. 2a), had a larger diameter: 40 ± 6 nm vs. 29 ± 5 nm, which indicated a more homogeneous and thicker TiO_2 coating.

The low magnification of the high resolution images (Fig. 3a and b) shows clearly the presence of the TiO_2 nanocrystals on the surfaces of the MWCNTs. HRTEM image indicates random orientation of the TiO_2 nanocrystals (Fig. 3c and d). Moreover, the observed crystallite sizes were similar to those obtained by XRD analysis. The surface of the MWCNT4 was decorated by TiO_2 nanoparticles that were intimately anchored to the oxidized MWCNT surface (Fig. 3c and d). The electron energy-loss spectrum, in the inset of Fig. 3d clearly shows the presence of a Ti L_{23} edge at 450 eV and an O K edge at 530 eV, indicating pure TiO_2 nanocrystals.

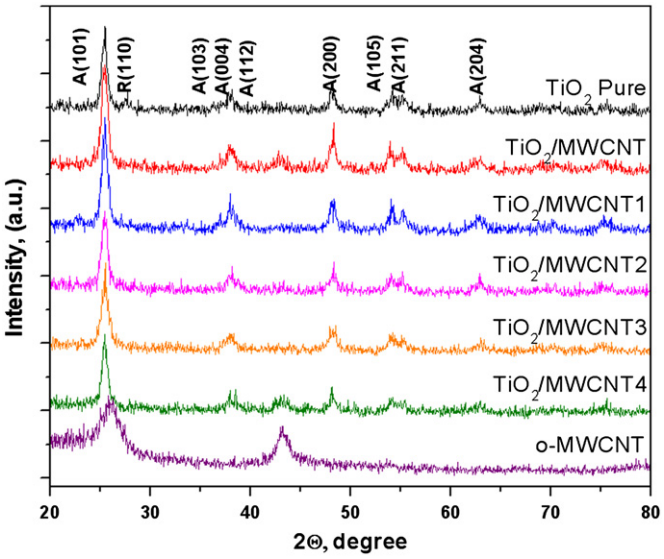

Fig. 1. XRD patterns of the synthesized photocatalysts.

Table 3
The mean crystallite size of anatase.

Sample	D_{mean} (nm)
TiO_2 Pure	14.0 ± 0.1
TiO_2/MWCNT	12.9 ± 0.3
TiO_2/MWCNT1	14.0 ± 0.2
TiO_2/MWCNT2	13.4 ± 0.4
TiO_2/MWCNT3	13.3 ± 0.5
TiO_2/MWCNT4	13.9 ± 0.4

3.2. Photocatalytic study

The change in the normalized dye concentration versus time is shown in Fig. 4, which reveals the significant influence of the oxidized MWCNTs on the photocatalytic activities of all the TiO_2 nanocomposites. The dye was completely degraded after 35 min in the presence of TiO_2/MWCNT4.

Three factors contributed to the enhanced photocatalytic activity: adsorption of the dye molecules, light absorption, and charge separation and transportation [14]. The adsorbtivity of the synthesized photocatalysts was related not only to physical adsorption, but also to the non-covalent π–π interaction of the dye molecules and the MWCNT surface [15]. According to the results of the photocatalytic studies and of the determination of the textural properties of the photocatalysts (Table 2), it could be concluded that the specific surface area, *i.e.* dye adsorption, is of lower significance for the enhancement of photocatalytic dye degradation. Similarly, Yan et al. [16] showed that the surface area of nanocrystalline TiO_2 catalysts with different anatase/rutile ratios is not a decisive factor in controlling the photocatalytic activity. Surface hybridization of TiO_2 with graphite-like carbon produced efficient photocatalysts due to high migration efficiency of the photo-induced electrons at the graphite-like carbon/TiO_2 interface, while only a small improvement of the adsorption properties of the catalyst in comparison to P25 was achieved [14]. The photocatalytic activity of graphene-supported TiO_2 nanocomposites with different graphene contents was mainly improved by the enhanced life-time of the photogenerated electron/hole pairs, and this property is almost independent of the surface area of the photocatalysts [17]. According to this, it could be supposed that the main role of the MWCNT derives from the pronounced electron-accepting character of the nanotube graphitic layer, which could contribute to a more effective charge separation and suppression of electron/hole pair recombination. The oxygen-containing functional groups at the TiO_2/MWCNT interface support the electron transporting properties of the nanocatalyst and this feature depends on their total acidity and functionality (Table 1). However, a comparison of the photocatalytic activities of all the nanocomposites and

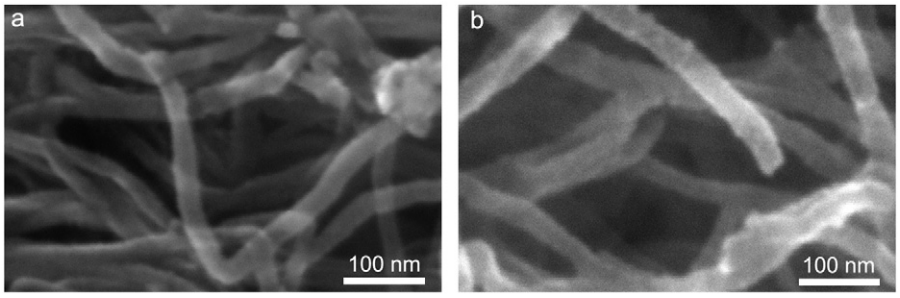

Fig. 2. FEG–SEM: (a) TiO_2/MWCNT and (b) TiO_2/MWCNT4 images of nanocomposites.

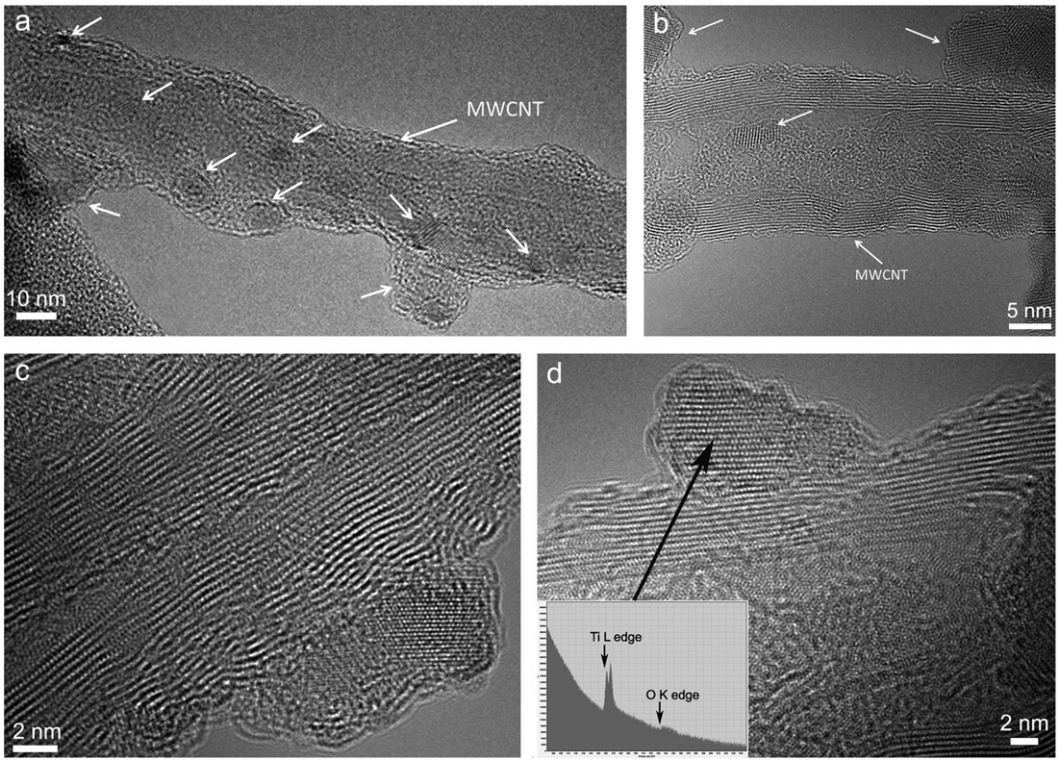

Fig. 3. TEM/HRTEM images of TiO_2/MWCNT4 nanocomposite (a and b)—the TiO_2 nanoparticles, marked by arrows, present on surface of MWCNT4; (c and d)—random orientation of the TiO_2 nanocrystals; EELS of TiO_2 crystallite—inset in (d).

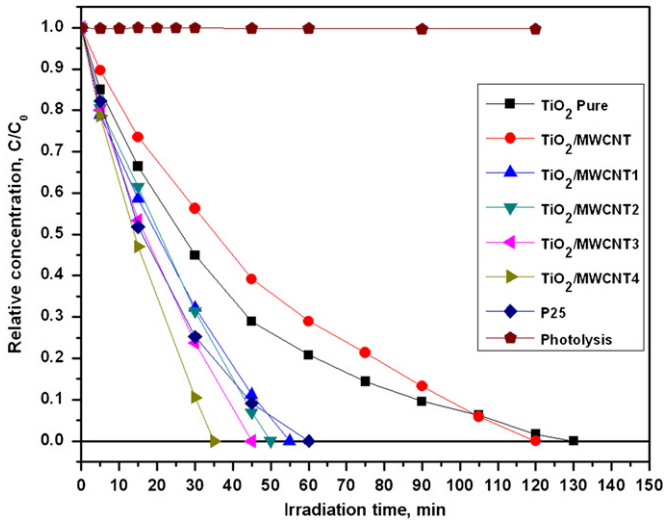

Fig. 4. Change in the relative dye concentration versus time for the synthesized photocatalysts.

pure TiO_2 leads to the conclusion that the synergetic effect of increased photogenerated electron/hole separation and specific surface area contributes to the increased photocatalytic dye degradation.

A study of the reusability of the photocatalysts showed that there was no significant decrease in the photodegradation efficiency for all catalysts (the overall decrease was in the range 2–5% of the initial), indicating good catalyst stability (Fig. 5). In addition to this, there were no significant differences in the photocatalytic activity of the TiO_2/MWCNT4 catalyst treated by simple washing or calcination between the consecutive reusability cycles (Fig. 5e). The heat treatment and washing of the catalyst between the cycles removed the dye degradation products from the catalyst surface and cavities resulting in recovery of the catalyst activity. Such result indicates that simple washing of the catalysts is an efficient and economical process for possible practical application of obtained photocatalysts.

4. Conclusions

The improved photocatalytic performance of the synthesized nanocomposite photocatalysts was obtained by hydrolysis of $TiBr_4$ and precipitation on differently oxidized MWCNTs. The oxidative treatment of the MWCNT introduced significant amounts of oxygen-containing functional groups, which played an important role in the nucleation and binding of TiO_2, thereby contributing to the increased photocatalytic activity of the synthesized nanocomposites. The TiO_2/MWCNT4 photocatalyst showed significant enhancement of photocatalytic degradation of the dye compared to P25 (enhancement factor 1.71) and the non-supported catalyst (3.71). Even higher values of enhancement factors of 2.04 and 4.42 were obtained when the active TiO_2 in the nanocomposites was considered, which undoubtedly confirmed significance of functionalized MWCNT support. It can be supposed

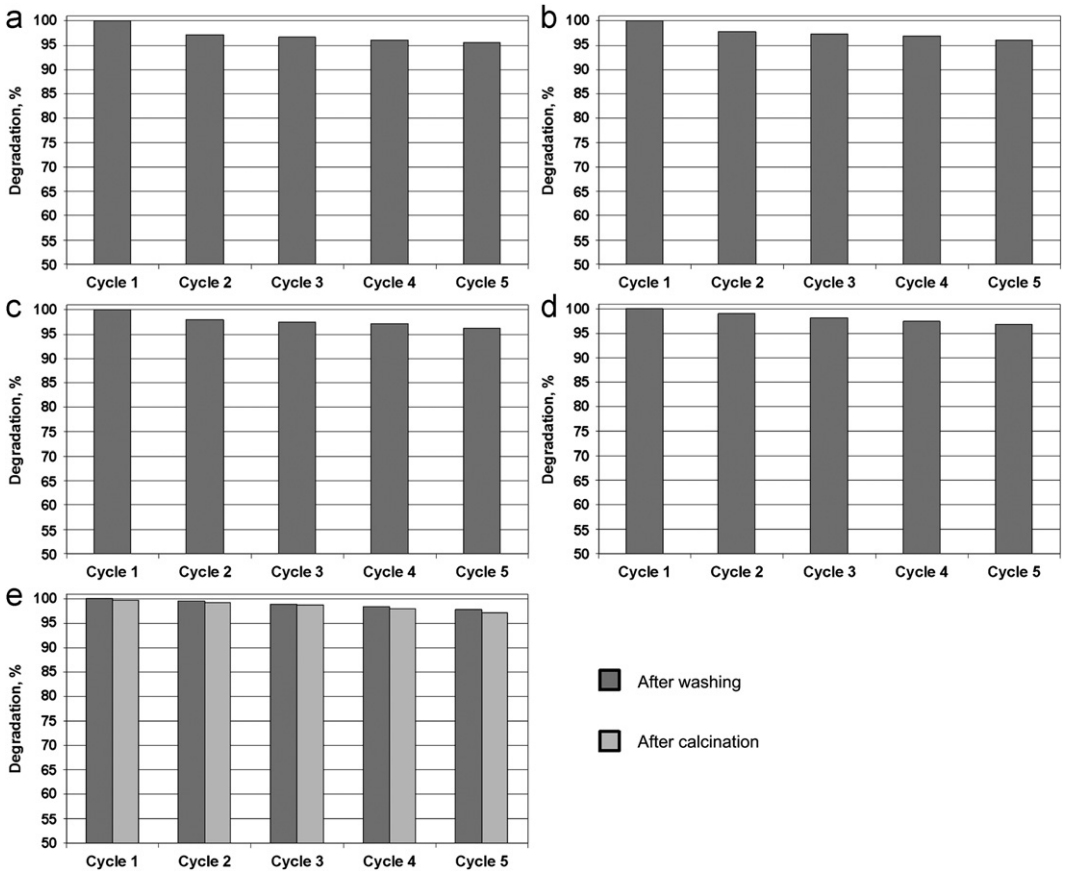

Fig. 5. Reusability of the synthesized photocatalysts: results of five repeated photocatalytic cycles under the same experimental conditions and appropriate irradiation time: (a) 120 min for TiO_2/MWCNT; (b) 55 min for TiO_2/MWCNT1; (c) 50 min for TiO_2/MWCNT2; (d) 45 min for TiO_2/MWCNT3 and (e) 35 min for TiO_2/MWCNT4.

that enhanced charge separation and transportation properties mainly contributed to the high photocatalytic activity of nanocomposites, as well as the increased specific surface area.

Acknowledgments

Financial support through the Ministry of Education and Science of the Republic of Serbia, Project no. III 45019 is gratefully acknowledged. V.R.R. would like to thank the FP7 NANOTECH FTM Project, Grant Agreement 245916, for financial support.

References

[1] A. Fujishima, K. Honda, Electrochemical photolysis of water at a semiconductor electrode, Nature 238 (1972) 37–38.
[2] N. Ruzycki, G.S. Herman, L.A. Boatner, U. Diebold, Scanning tunneling microscopy study of the anatase (1 0 0) surface, Surface Science Letters 529 (2003) 239–244.
[3] K. Woan, G. Pyrgiotakis, W. Sigmund, Photocatalytic carbon-nanotube–TiO_2 composites, Advanced Materials 21 (2009) 2233–2239.
[4] G. Socol, Yu. Gnatyuk, N. Stefan, N. Smirnova, V. Djokić, C. Sutan, V. Malinovschi, A. Stanculescu, O. Korduban, I.N. Mihailescu, Photocatalytic activity of pulsed laser deposited TiO_2 thin films in N_2, O_2 and CH_4, Thin Solid Films 518 (2010) 4648–4653.
[5] R. Leary, A. Westwood, Carbonaceous nanomaterials for the enhancement of TiO_2 photocatalysis, Carbon 49 (2011) 741–772.
[6] K.A. Wepasnick, B.A. Smith, K.E. Schrote, H.K. Wilson, S.R. Diegelman, D.H. Fairbrother, Surface and structural characterization of multi-walled carbon nanotubes following different oxidative treatments, Carbon 49 (2011) 24–36.
[7] J.P. Chen, S. Wu, Acid/base-treated activated carbons: characterization of functional groups and metal adsorptive properties, Langmuir 20 (2004) 2233–2242.
[8] A.J. Plomp, D.S. Su, K.P. de Jong, J.H. Bitter, On the nature of oxygen-containing surface groups on carbon nanofibers and their role for Platinum deposition—an XPS and Titration study, Journal of Physical Chemistry C 113 (2009) 9865–9869.
[9] H.F. Gorgulho, J.P. Mesquita, F. Gonçalves, M.F.R. Pereira, J.L. Figueiredo, Characterization of the surface chemistry of carbon materials by potentiometric titrations and temperature-programmed desorption, Carbon 46 (2008) 1544–1555.
[10] Z. Németh, C. Dieker, Á. Kukovecz, D. Alexander, L. Forró, J.W. Seo, K. Hernadi, Preparation of homogeneous titania coating on the surface of MWNT, Composites Science & Technology 71 (2011) 87–94.
[11] B.W. Smith, D.E. Luzzi, Electron irradiation effects in single wall carbon nanotubes, Journal of Applied Physics 90 (2001) 3509–3606.
[12] H.P. Boehm, in: D.D. Eley, H. Pines, P.B. Weisz (Eds.), Advances in Catalysis, vol. 16, Academic Press, New York, 1966, pp. 179–274.
[13] C. Lu, C. Chiu, Adsorption of zinc(II) from water with purified carbon nanotubes, Chemical Engineering Science 61 (2006) 1138–1145.
[14] L.W. Zhang, H.B. Fu, Y.F. Zhu, Efficient TiO_2 photocatalysts from surface hybridization of TiO_2 particles with graphite-like carbon, Advanced Functional Materials 18 (2008) 2180–2189.

[15] J. Ma, R. Xiao, J. Li, J. Yu, Y. Zhang, L. Chen, Determination of 16 polycyclic aromatic hydrocarbons in environmental water samples by solid-phase extraction using multi-walled carbon nanotubes as adsorbent coupled with gas chromatography–mass spectrometry, Journal of Chromatography A 1217 (2010) 5462–5469.
[16] M. Yan, F. Chen, J. Zhang, M. Anpo, Preparation of controllable crystalline Titania and study on the photocatalytic properties, Journal of Physical Chemistry B 109 (2005) 8673–8678.
[17] Y. Zhang, Z.-R. Tang, X. Fu, Y.-J. Xu, Engineering the unique 2D mat of graphene to achieve graphene–TiO_2 nanocomposite for photocatalytic selective transformation: what advantage does graphene have over its forebear carbon nanotube?, ACS Nano 5 (2011) 7426–7435.